

SUPPORTING INFORMATION

Nanostar clustering improves the sensitivity of plasmonic assays

Yong Il Park, Hyungsoon Im, Ralph Weissleder and Hakho Lee

Table of Contents

Experimental procedures.....	S2
Figure S1. Size distribution of AuNS measured by DLS	S4
Figure S2. TEM images of AuNS with different sizes and shapes	S5
Figure S3. Plot of LSPR peak width as a function of the AuNS size.....	S6
Figure S4. Stability of AuNS.....	S7
Figure S5. FDTD simulation of AuNS dimer in different configurations.....	S8
Figure S6. Size distribution of AuNS clusters measured by DLS	S9
Figure S7. Light scattering from individual and clustered AuNS.....	S10
Figure S8. Titration data of KIM1 antibody-conjugated AuNS	S11
Figure S9. FDTD simulation of AuNS dimer as a function of inter-particle distance	S12
Table S1. Estimated inter-particle distances depending on the ligand	S13
Supplementary references.....	S14

EXPERIMENTAL PROCEDURES

Materials. Gold(III) chloride trihydrate ($\geq 99.9\%$), silver nitrate ($\geq 99.0\%$), ascorbic acid, sodium citrate dihydrate ($\geq 99\%$), 11-mercaptoundecanoic acid (MUA), 2-mercaptoethylamine (MEA), 2-maleimidoethylamine trifluoroacetate salt ($\geq 95\%$) were purchased from Sigma-Aldrich. 40 nm spherical gold nanoparticles were purchased from nanoComposix, inc. Methyl-PEG₄-thiol (MT(PEG)₄), 1-ethyl-3-(3-dimethylaminopropyl)carbodiimide hydrochloride (EDC), N-hydroxysulfosuccinimide (sulfo-NHS), (+)-biotinyl-3,6,9-trioxaundecanediamine (amine-PEG₃-biotin), neavidin protein were purchased from Thermo Scientific. Human KIM1 polyclonal antibody, recombinant human KIM1, normal goat IgG control were purchased from R&D Systems.

Synthesis of gold nanoparticles. The star-shaped gold nanoparticles (Gold nanostars, AuNS) were synthesized using a seed-mediated growth method, as previously reported.¹ First, the seed gold nanoparticles were prepared through citrate reduction of HAuCl₄ by the Turkevich method.² Sodium citrate (38.8 mM, 50 mL) was added to the boiling HAuCl₄ solution (1 mM, 500 mL) under vigorous stirring, and the mixture was refluxed for 15 min. The seed particles (200 μ L) were then added to HAuCl₄ (0.25 mM, 10 mL) containing HCl (1 M, 10 μ L). AgNO₃ (2 mM, 100 μ L) and ascorbic acid (0.1 M, 50 μ L) were sequentially added to the mixture to initiate the particle growth. The reaction was completed in 30 sec, and the as-synthesized AuNS were purified by centrifugation. The precipitated AuNS were redispersed in 8 mL distilled water. The size of AuNS could be controlled by changing the seed amount. Decreasing seed particle concentrations resulted in larger AuNS. The surface of bare AuNS was functionalized with carboxylic acid. NaOH solution (0.5 M, 80 μ L) was added to 8 mL of AuNS solution. Then, MUA (20 mM, 0.4 mL in ethanol) and MT(PEG)₄ (20 mM, 0.4 mL in ethanol) were added to the AuNS solution under stirring. After overnight incubation, the functionalized AuNS were washed twice and then dispersed in 1 mL distilled water (~ 1 nM AuNS). The MUA allows to covalently conjugate affinity ligands through EDC coupling and the PEG layer improves surface hydrophilicity and reduces non-specific binding. The size and shape of the AuNS were characterized by using transmission electron microscopy (TEM, JEOL 2100). The number of the AuNS was counted by nanoparticle tracking analysis (NTA). The hydrodynamic size of the AuNS was measured by dynamic light scattering (Zetasizer APS).

Refractive index sensitivity. The refractive index sensitivities (RIS) of the AuNS and AuNP were measured by incubating the nanoparticles in solvents with different refractive indices (n). The solvents were prepared by mixing DMSO ($n = 1.48$) and water ($n = 1.33$) at different volume ratios. The absorbance spectra of the samples were measured by a microplate reader (Tecan Safire2™). Figure of merit (FOM) was calculated as a ratio of the measured RIS to the full width at half maximum (FWHM) of the corresponding peak.

Preparation of biotinylated gold nanoparticles. EDC (4 mg/mL, 10 μ L) and amine-PEG₃-biotin (10 mg/mL, 100 μ L) were added to 1 mL of nanoparticle solution, and the mixture was incubated for 2 hrs at room temperature. The particles were washed twice via centrifugation (3000 \times g), and dispersed in 1 mL of 10 mM phosphate buffered saline (PBS) solution.

Antibody conjugation. AuNS conjugated with full polyclonal antibodies were prepared by EDC coupling between AuNS and antibodies. EDC (4 mg/mL, 20 μ L) and sulfo-NHS (11 mg/mL, 20 μ L) were

added to 1 mL of nanoparticle solution. The solution was incubated for 15 min at room temperature, and then washed via centrifugation ($3000 \times g$, $4\text{ }^{\circ}\text{C}$). The activated nanoparticles were dispersed in 1 mL of 10 mM PBS. Antibody (1mg/mL, $20\text{ }\mu\text{L}$) was mixed with the activated nanoparticles (0.5 mL), and incubated for 2 hrs at room temperature. The antibody conjugated AuNS were purified by centrifugation ($3000 \times g$), and dispersed in 1 mL of 10 mM PBS. For conjugation with half-antibody fragments, the surface of AuNS was functionalized by maleimide group to make a thioether bond between AuNS and antibody fragments. EDC (4 mg/mL, $20\text{ }\mu\text{L}$) and sulfo-NHS (11 mg/mL, $20\text{ }\mu\text{L}$) were added to 1 mL of nanoparticle solution. The reaction solution was incubated for 15 min at room temperature, and then washed twice. 2-maleimidoethylamine (1 mg/mL, 0.25 mL) was added to the AuNS solution, and reacted for 2 hrs at room temperature. After repeated washing, the nanoparticles were dispersed in 1 mL of 10 mM PBS. Thiolated antibody was prepared by cleaving hinge region disulfide bonds in the heavy chains. Antibody (1mg/mL, $30\text{ }\mu\text{L}$) was mixed with MEA (60 mg/mL, $3\text{ }\mu\text{L}$), and incubated for 90 min at $37\text{ }^{\circ}\text{C}$. The thiolated antibody was purified using Zeba™ spin desalting column (7k MWCO, Thermo Scientific), and added to maleimide-AuNS. Following the incubation overnight at $4\text{ }^{\circ}\text{C}$, the conjugated AuNS were purified by centrifugation, and dispersed in 1 mL of 10 mM PBS.

Titration experiments. Neutravidin solutions ($5\text{ }\mu\text{L}$) at different concentration were mixed with the biotinylated 70 nm AuNS ($45\text{ }\mu\text{L}$, 0.2 nM) and 40 nm AuNP ($45\text{ }\mu\text{L}$, 0.2 nM), and incubated for 30 min at room temperature. 40 nm AuNP was chosen for comparison with AuNS because they have similar particle volume. Three duplicated samples were prepared for triplicate measurements. The absorbance spectra of the samples on a 384 well plate were measured by a microplate reader (Tecan Safire2™). For antibody experiment, KIM1 solutions ($5\text{ }\mu\text{L}$) at different concentration were mixed with AuNS probes ($45\text{ }\mu\text{L}$), and reacted for 30 min at room temperature. Same procedure used in the neutravidin experiment was applied for KIM1 detection. The limit of detection (LOD) was obtained from the titration curve as $3 \times$ standard deviation (s.d.) of background signal.

LSPR analysis. LSPR peak positions were calculated using a custom-built Matlab software by fitting the absorbance peak to a polynomial curve.³ All measurements were performed in triplicate and the data are displayed as mean \pm s.d.

FDTD simulations. 3-dimensional finite-difference time-domain (FDTD) simulations were performed using a commercial software package (FDTD solutions, Lumerical). The dimensions of spherical and star nanoparticles were obtained from TEM images (**Figure S2**). The extinction spectra, field intensity and spectral shift were calculated from a unit cell with a single nanoparticle or dimer. A non-uniform mesh with a minimum grid size of 1 nm was used. The dielectric constants for Au were obtained from reference.⁴ The refractive index of the molecules and ligands was set to 1.6.

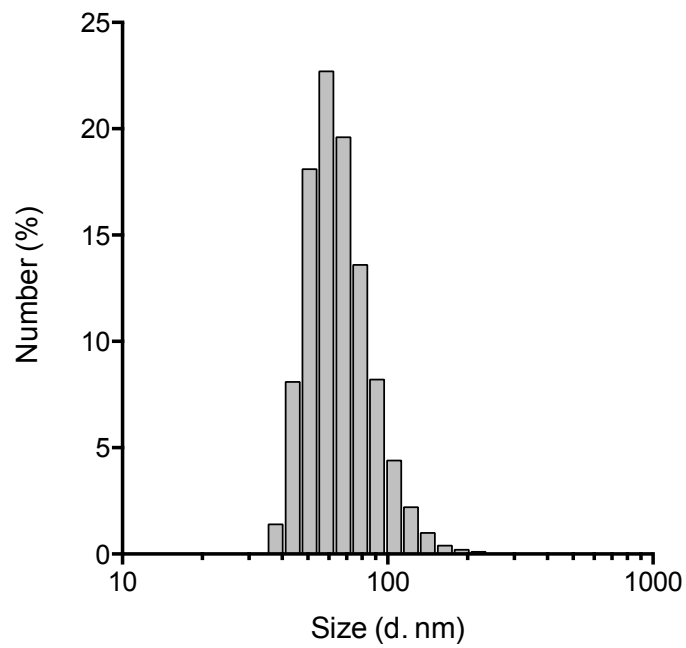
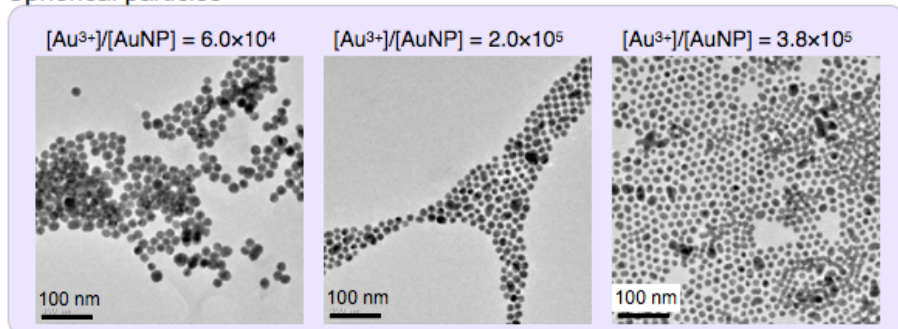
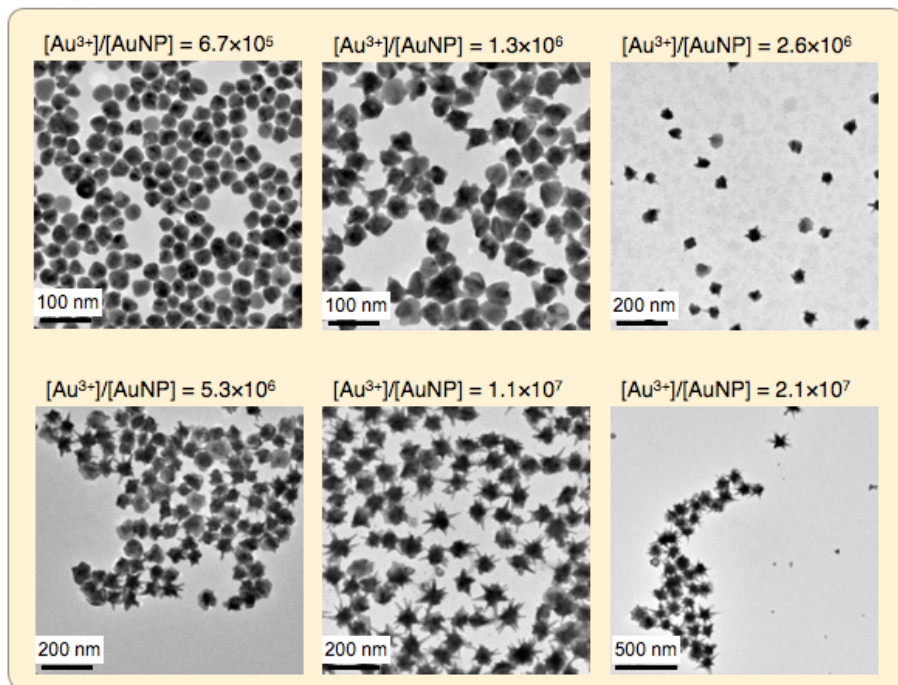


Figure S1. Size distribution of AuNS measured by DLS. The hydrodynamic size of AuNS was 68.18 ± 21.76 nm.

Spherical particles



Nanostars



Mixed phase

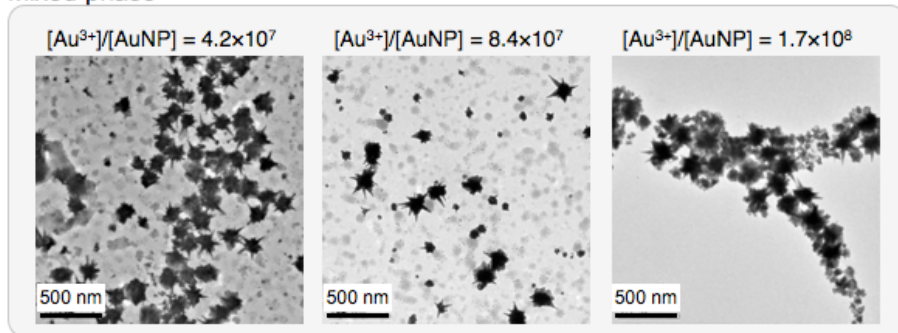


Figure S2. TEM images of AuNS with different sizes and shapes. When $[\text{Au}^{3+}]/[\text{AuNP}]$ ratio was $< 4 \times 10^5$, the seeds becomes bigger AuNPs rather than AuNS (upper row). As the ratio increases, larger AuNS was synthesized (middle row). When the ratio was $> 2 \times 10^7$, the AuNP separately nucleated with AuNS growth, resulting in the mixture of AuNS and AuNP (bottom row).

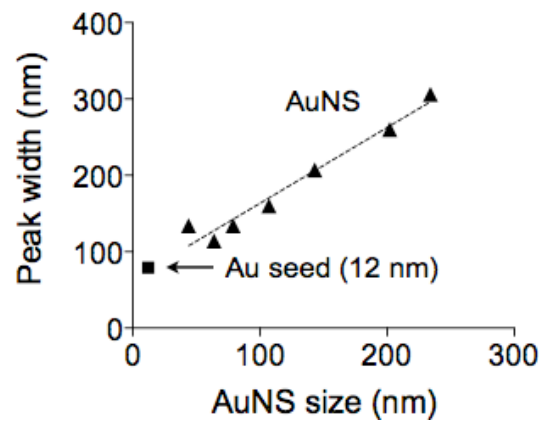


Figure S3. Plot of LSPR peak width as a function of the AuNS size. The spectrum peak width linearly increases with the AuNS size.

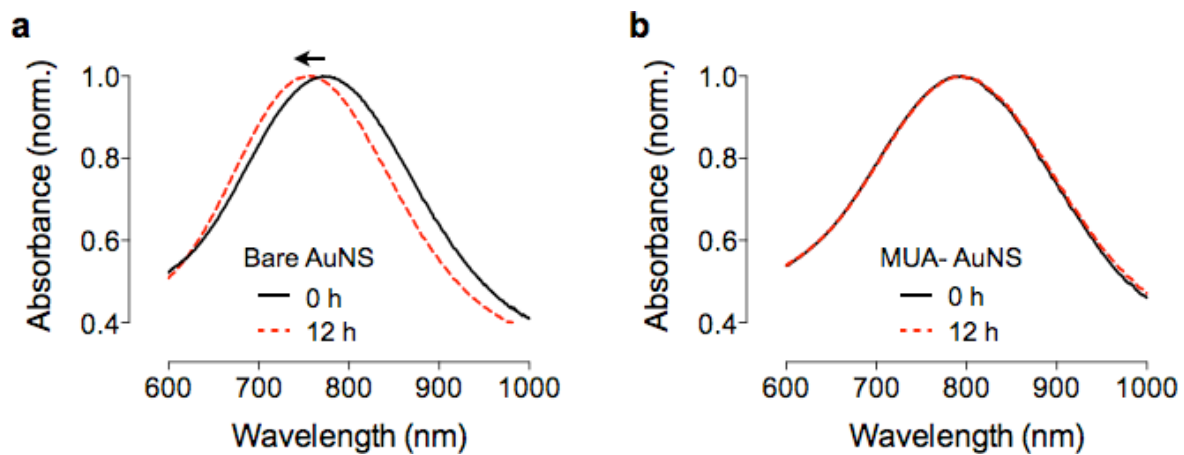


Figure S4. Stability of AuNS. (a) As-synthesized bare AuNS showed a drift of peak position to a shorter wavelength. A 15 nm of blue shift of the peak was observed after 12 hrs. (b) The MUA coated AuNS was stable with no shift observed after 12 hrs.

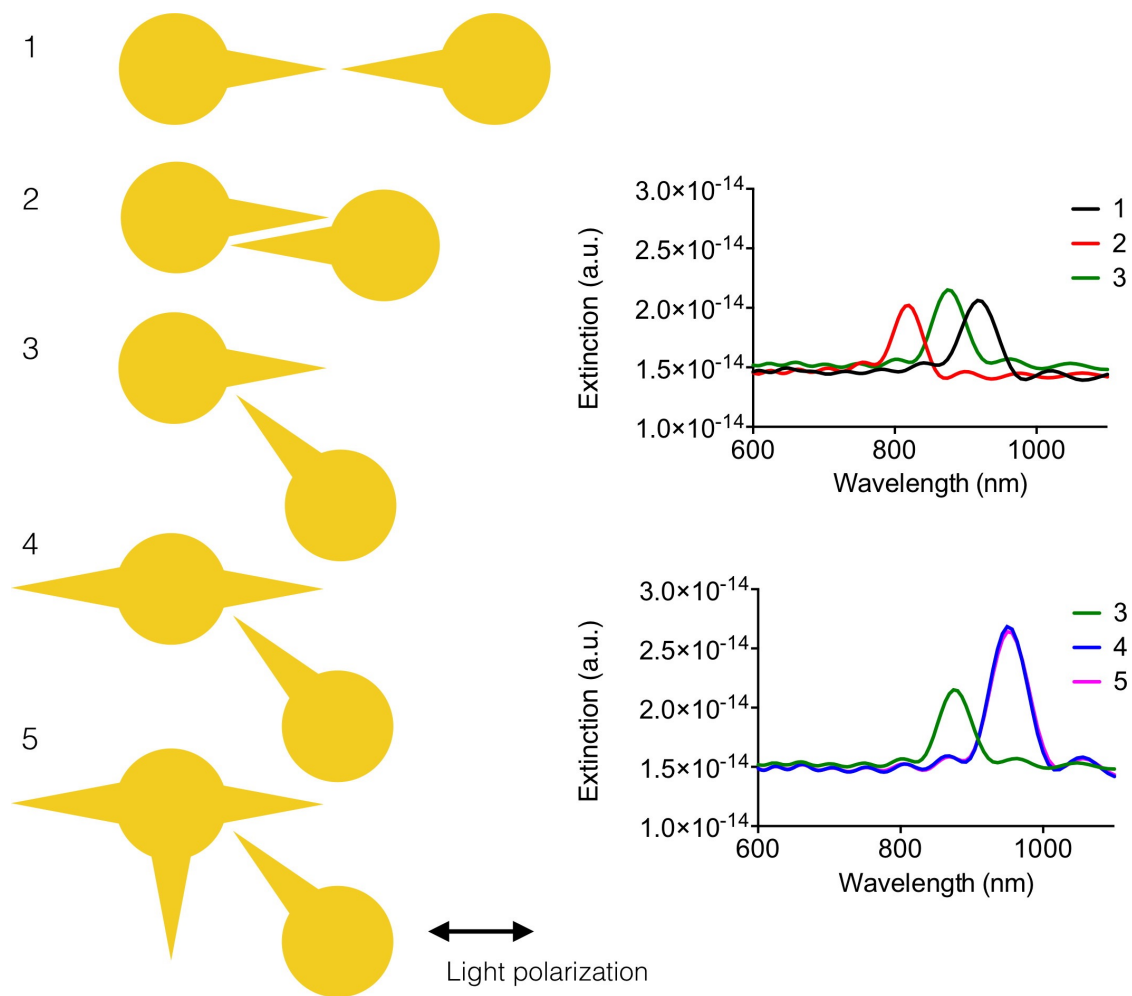


Figure S5. FDTD simulation of AuNS dimer in different configurations. The maximum spectral shift can be achieved when the tips of the AuNS dimer aligned along the direction of incident light polarization. Misaligned tips did not contribute to a spectral shift when a dimer formed.

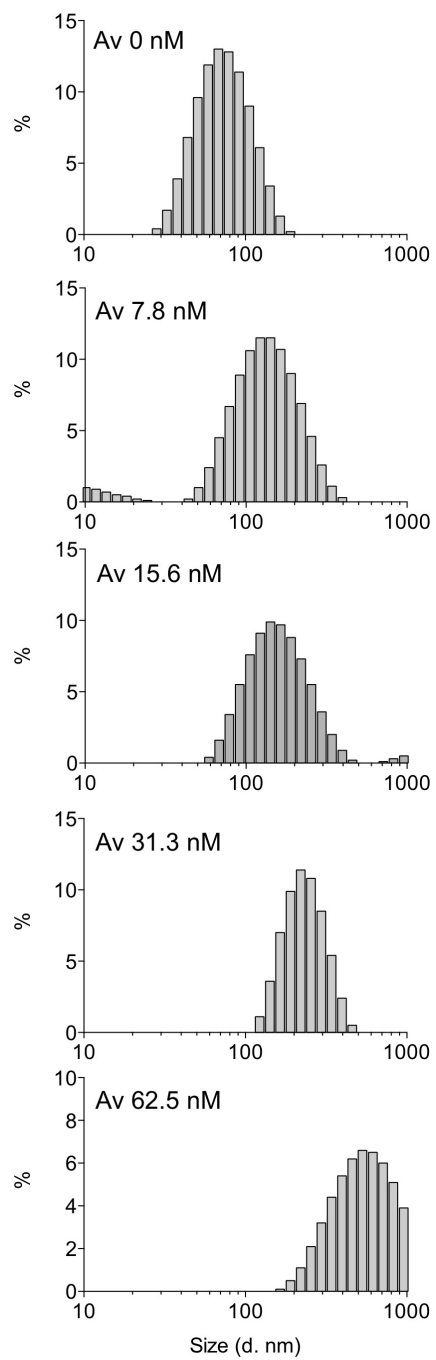


Figure S6. Size distribution of AuNS clusters measured by DLS. The size change of AuNS clusters through avidin-biotin interaction was monitored.

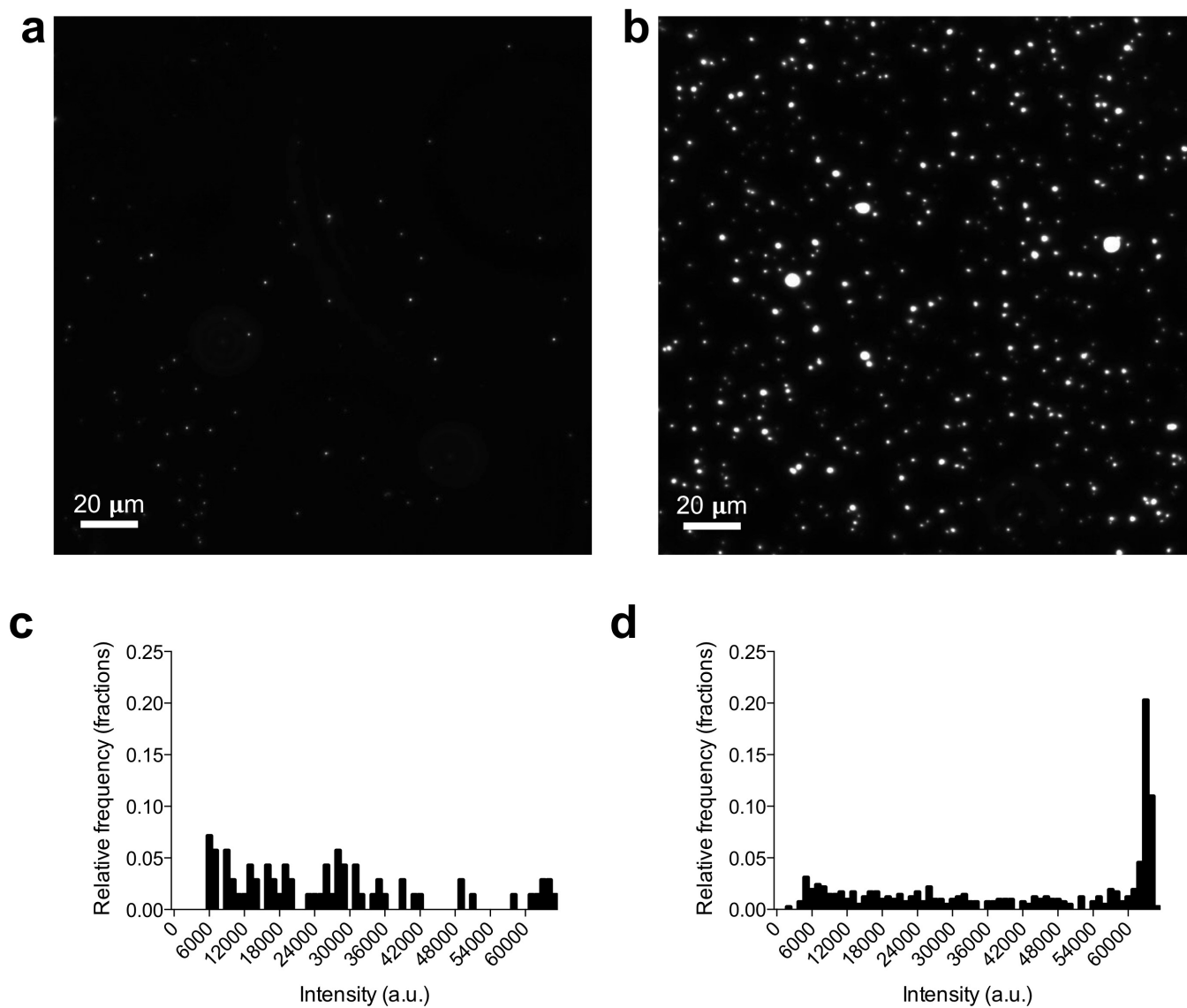


Figure S7. Light scattering from individual and clustered AuNS. Light scattering images from (a) individual biotinylated AuNS and (b) clustered AuNS through avidin-biotin interaction. Intensity histogram of (c) individual biotinylated AuNS and (d) clustered AuNS from light scattering images (a and b). This microscopic method could be sensitive in detecting AuNS clusters.⁵ However, the assay speed and throughput would be limited and requires high magnification (to resolve individual clusters) and multiple image acquisitions (due to a smaller field of view). Conversely, the absorption-based detection is simple and scalable for high throughput assay, as it measures signal from bulk samples on a microplate-reader format.

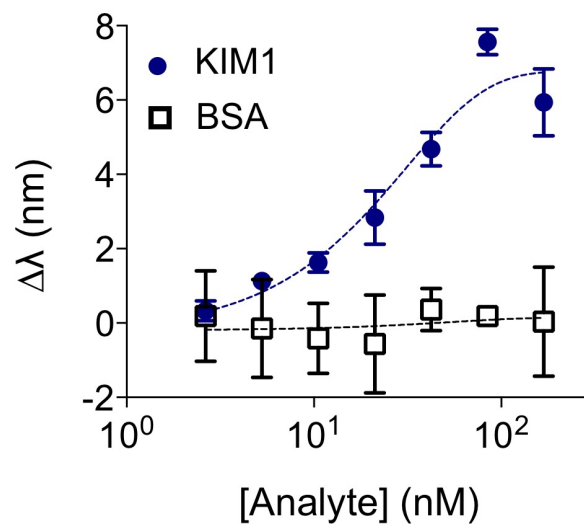


Figure S8. Titration data of KIM1 antibody-conjugated AuNS. To rule out non-specific aggregation, BSA was also used as a control analyte. We observed negligible signal changes even at high BSA dose, which confirmed the signal changes are due to antibody-antigen specific aggregation.

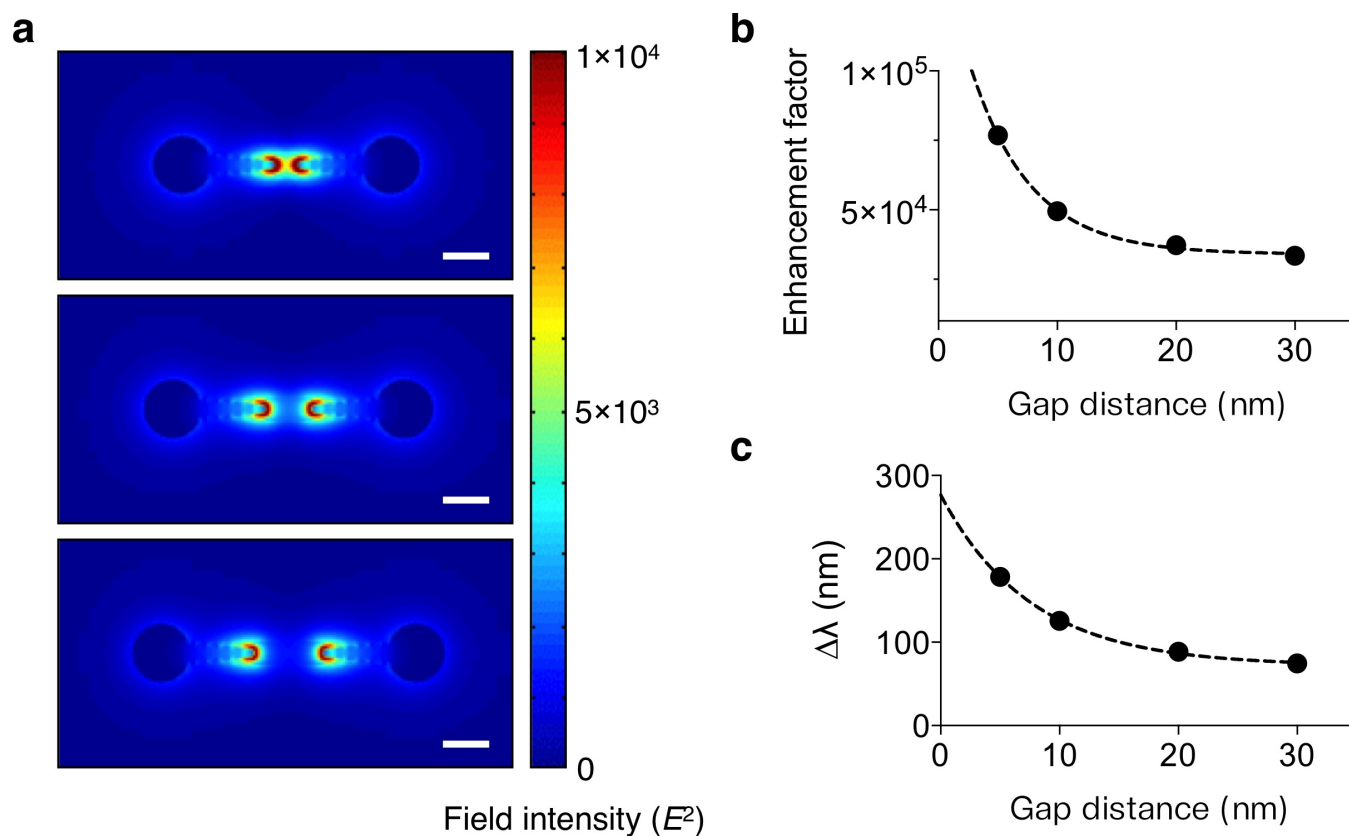


Figure S9. FDTD simulation of AuNS dimer as a function of inter-particle distance. (a) Simulated electric field (E) distribution surrounding a AuNS dimer at varying inter-particle distance. The field enhancement inversely depends on the inter-particle distance (d_{pp}). Scale bar, 50 nm. (b-c) Field enhancement factor and corresponding spectral shift decrease exponentially with d_{pp} .

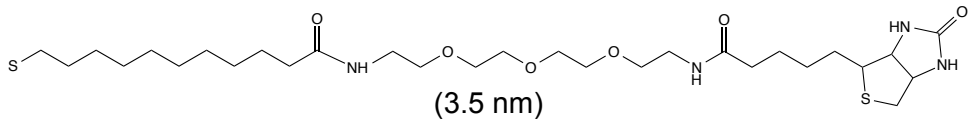
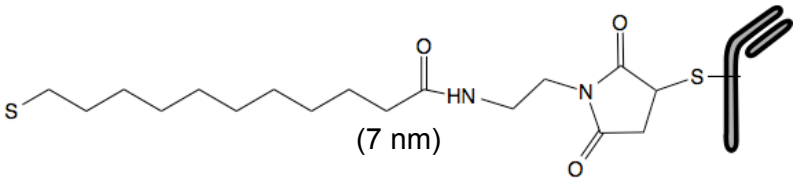
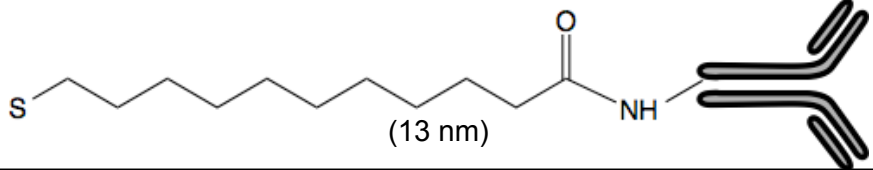
Detection model	Ligand on AuNS (size)	Target (size)
Avidin & Biotin	 (3.5 nm)	Avidin (7 nm)
Half antibody & protein	 (7 nm)	KIM1 (7 nm)
Full antibody & protein	 (13 nm)	KIM1 (7 nm)

Table S1. Estimated inter-particle distances depending on the ligand. The length of biotin linker was estimated from the manufacturer (<http://www.piercenet.com/product/ez-link-amine-peg-biotin-reagents>). The avidin and antibody sizes were estimated from the references.^{6,7} KIM1 antigen size was assumed to be the same as the avidin size.

SUPPLEMENTARY REFERENCES

- (1) Yuan, H., Khoury, C. G., Hwang, H., Wilson, C. M., Grant, G. A., and Vo-Dinh, T. (2012) Gold nanostars: surfactant-free synthesis, 3D modelling, and two-photon photoluminescence imaging. *Nanotechnology* 23, 075102.
- (2) Turkevich, J., Stevenson, P. C., and Hillier, J. (1951) A Study of the Nucleation and Growth Processes in the Synthesis of Colloidal Gold. *Disc. Faraday Soc.* 55-75.
- (3) Im, H., Sutherland, J. N., Maynard, J. A., and Oh, S. H. (2012) Nanohole-based surface plasmon resonance instruments with improved spectral resolution quantify a broad range of antibody-ligand binding kinetics. *Anal. Chem.* 84, 1941-1947.
- (4) Palik, E. D. (1998) *Handbook of optical constants of solids*. <http://www.sciencedirect.com/science/book/9780125444156>, Elsevier.
- (5) Bu, T., Zako, T., Fujita, M., and Maeda, M. (2013) Detection of DNA induced gold nanoparticle aggregation with dark field imaging. *Chem. Commun.* 49, 7531-7533.
- (6) Berndt, M., Lorenz, M., Enderlein, J., and Diez, S. (2003) Axial nanometer distances measured by fluorescence lifetime imaging microscopy. *Nano Lett.* 10, 1497-1500.
- (7) Tan, Y. H., Liu, M., Nolting, B., Go, J. G., Gervay-Hague, J., and Liu, G.-y. (2008) A nanoengineering approach for investigation and regulation of protein immobilization. *ACS Nano* 2, 2374-2384.